

Chapter 4

RET of Rarefied Monatomic Gas

Abstract In this chapter, we give a survey of the main results of RET concerning rarefied monatomic gases, some of which are explained in the Müller–Ruggeri book of RET (Müller and Ruggeri, *Rational Extended Thermodynamics*, Springer, New York, 1998). We start from the phenomenological RET theory with 13 fields and prove that the closure of RET coincides with the one obtained by Grad using kinetic arguments and with the MEP procedure. The theory with N -moments is also presented with the proof of nesting theories that emerge from the concept of principal subsystem. The problematic of bounded domain in RET is also considered, and a simple example of heat conduction is explained to show a significant difference of the results between RET and NSF.

A lower bound for the maximum characteristic velocity is obtained in terms of the truncation tensor index N . This quantity increases as the number of moments grows and it is unbounded when $N \rightarrow \infty$.

The relativistic counterpart is also described briefly. In this framework, the maximum characteristic velocity is bounded for any number of moments, and converges to the light velocity from the below for $N \rightarrow \infty$.

The chapter contains also comparison between the RET theory and experiments in sound waves and light scattering.

4.1 Extended Thermodynamics with 13 Fields and Subsystems

We saw, in Sect. 1.5.1, that RET of rarefied monatomic gases is intimately related to the moment theory (1.18) associated with the Boltzmann equation. As emphasized there, the 13-field RET theory is a purely phenomenological theory [1] in which the system of field equations in balance type (1.24) is adopted and the closure of the system with the use of the universal principles of physics is accomplished. We saw also, in Sect. 1.5.2, the problem of closure of the 13-moment theory.

We have three closure methods by using the universal principles of macroscopic ET [1], the perturbative method of Grad [2] at the kinetic level, and the maximum entropy principle [3]. The vital point is that three different and apparently uncorrelated closure methods give the same system (1.25).

The differential system (1.25) has been extensively studied. For example, acceleration waves, shock waves, shock wave structure, and the hyperbolicity region were studied (for details see [4] and references therein).

In this section we summarize the 13-moment system and its principal subsystems.

The equations of ET with 13 fields are given in (1.25). The components of the main field \mathbf{u}' :

$$\mathbf{u}' \equiv (\lambda, \lambda_i, \mu, \lambda_{\langle ij \rangle}, \mu_i)$$

have the following expressions [4, 5]:

$$\begin{aligned} \lambda &= -\frac{1}{T} \left\{ g - \frac{v^2}{2} + \frac{1}{2p} \sigma_{\langle ij \rangle} v_i v_j - \frac{\rho}{5p^2} q_i v_i v^2 \right\}, \\ \lambda_i &= -\frac{1}{T} \left\{ v_i - \frac{1}{p} \sigma_{\langle ij \rangle} v_j + \frac{\rho}{5p^2} (v^2 q_i + 2q_j v_j v_i) - \frac{q_i}{p} \right\}, \\ \mu &= \frac{1}{2T} \left\{ 1 - \frac{2\rho}{3p^2} q_k v_k \right\}, \\ \lambda_{\langle ij \rangle} &= \frac{1}{T} \left\{ \frac{1}{2p} \sigma_{\langle ij \rangle} + \frac{\rho}{5p^2} \left(v_i q_j + v_j q_i - \frac{2}{3} v_k q_k \delta_{ij} \right) \right\}, \\ \mu_i &= -\frac{\rho}{5Tp^2} q_i. \end{aligned} \quad (4.1)$$

The maximum characteristic velocity in equilibrium is $\lambda_{\max} = 1.65c_0$ (c_0 is the sound velocity for a monatomic gas).

Let us consider possible principal subsystems following the general theory presented in Sect. 2.4.

4.1.1 10-Field Principal Subsystem

The 10-field system is a principal subsystem of the 13-field system when

$$\mu_i = 0 \quad \rightarrow \quad q_i = 0.$$

Neglecting the last block of the corresponding equation of (1.25) and inserting $q_i = 0$ in the previous equations, we have

$$\begin{aligned} \frac{\partial \rho}{\partial t} + \frac{\partial}{\partial x_k} (\rho v_k) &= 0, \\ \frac{\partial \rho v_i}{\partial t} + \frac{\partial}{\partial x_k} \{ \rho v_i v_k + p \delta_{ik} - \sigma_{\langle ik \rangle} \} &= 0, \end{aligned}$$

$$\begin{aligned}
& \frac{\partial}{\partial t} (\rho v^2 + 2\rho\varepsilon) + \frac{\partial}{\partial x_k} \{ \rho v^2 v_k + 2(\rho\varepsilon + p)v_k - 2\sigma_{\langle kl \rangle} v_l \} = 0, \\
& \frac{\partial}{\partial t} \{ \rho v_i v_j + p\delta_{ij} - \sigma_{\langle ij \rangle} \} + \\
& \frac{\partial}{\partial x_k} \left\{ \rho v_i v_j v_k + p(v_i\delta_{jk} + v_j\delta_{ki} + v_k\delta_{ij}) - \sigma_{\langle ij \rangle} v_k - \sigma_{\langle jk \rangle} v_i - \sigma_{\langle ki \rangle} v_j \right\} = \frac{\sigma_{\langle ij \rangle}}{\tau_S}.
\end{aligned} \tag{4.2}$$

In this case $\lambda_{\max} = 1.34c_0$.

4.1.2 Euler 5-Field Principal Subsystem

The Euler system is the 5-field principal subsystem of the 13- and 10-field systems when

$$\mu_i = 0, \quad \lambda_{\langle ij \rangle} = 0 \rightarrow q_i = 0, \quad \sigma_{\langle ij \rangle} = 0.$$

Neglecting the last block of the corresponding equation of (4.2), and inserting $\sigma_{\langle ij \rangle} = 0$, in the previous equations, we have

$$\begin{aligned}
& \frac{\partial \rho}{\partial t} + \frac{\partial}{\partial x^k} (\rho v_k) = 0, \\
& \frac{\partial \rho v_i}{\partial t} + \frac{\partial}{\partial x^k} (\rho v_i v_k + p\delta_{ik}) = 0, \\
& \frac{\partial}{\partial t} (\rho v^2 + 2\rho\varepsilon) + \frac{\partial}{\partial x_k} \{ \rho v^2 v_k + 2(\rho\varepsilon + p)v_k \} = 0.
\end{aligned} \tag{4.3}$$

The maximum velocity is now $\lambda_{\max} = 1 c_0$.

4.1.3 4-Field Principal Subsystem

The so called p -system is the 4-field subsystem of the Euler system (4.3) with

$$\mu_i = 0, \quad \lambda_{\langle ij \rangle} = 0, \quad \mu = \text{const.} \rightarrow q_i = 0, \quad \sigma_{\langle ij \rangle} = 0, \quad T = T^* = \text{const.}$$

The system of field equations is given by

$$\frac{\partial}{\partial t} \rho + \frac{\partial}{\partial x^i} (\rho v_i) = 0,$$

$$\frac{\partial}{\partial t} (\rho v_j) + \frac{\partial}{\partial x^i} (\rho v_i v_j + p^* \delta_{ij}) = 0,$$

where

$$p^* \equiv p(\rho, T^*) \quad \text{and} \quad \lambda_{\max} = 0.7746 c_0 .$$

4.1.4 1-Field Principal Subsystem

Finally, the transport equation:

$$\frac{\partial}{\partial t} \rho + \frac{\partial}{\partial x^i} (\rho v_i^*) = 0$$

is a 1-field principal subsystem of all the previous ones:

$$\begin{aligned} \mu_i &= 0, \quad \lambda_{<ij>} = 0, \quad \mu = \text{const.}, \quad \lambda_j = \text{const.} \rightarrow \\ q_i &= 0, \quad \sigma_{<ij>} = 0, \quad T = T^* = \text{const.}, \quad v_i = v_i^* = \text{const.} \end{aligned}$$

and we have $\lambda_{\max} = 0$.

According with the general result, the maximum characteristic velocity increases with the number of fields [6].

4.2 Bounded Domain: Heat Conduction and Problematic Boundary Data

Up to here, we have considered phenomena evolving in an unbounded domain and we have seen that ET is successful because (1) it satisfies explicitly the universal principles of physics, (2) it has a desired mathematical structure of symmetric hyperbolic systems, (3) it is perfectly consistent with the kinetic theory, and (4) the results derived from it are in good agreement with experimental data. The analysis of phenomena in a bounded domain is, however, not quite satisfactory when the number of moments is more than 13 as we will see below.

In this section, we summarize the problems encountered in the study of nonequilibrium phenomena in a bounded domain. Let us start with the heat-conduction

problem by using the 13-moment ET theory. We will see that the results in non-planar geometry are very different from the results predicted by the classical Navier-Stokes Fourier theory.

4.2.1 Heat Conduction Analyzed by the 13-Moment ET Theory

Müller and Ruggeri [7] studied one-dimensional heat conduction in a gas at rest in planar, cylindrical and spherical geometries by using the 13-moment ET theory. It turns out that, in the radially symmetric cases, the stress tensor does not reduce to a scalar pressure and that the heat flux depends on the normal components of the deviatoric stress tensor. As a result, the singularities of temperature on the axis of the cylinder and in the center of the sphere—which are characteristic for the Navier-Stokes Fourier solution—disappear. In this section, we explain this result.

For the present argument the nature of the molecular interaction is quite irrelevant. Therefore we choose the simplest model and consider the system of equations based upon the BGK model. Furthermore, we spread out the covariant derivatives by using the Christoffel symbols. Then we obtain a more specific, but more complex version of the field equations (1.25), which in a stationary case becomes [7]:

$$\begin{aligned}
 g^{ik} \frac{\partial p}{\partial x^k} - \frac{\partial \sigma^{<ik>}}{\partial x^k} - \Gamma_{kl}^i \sigma^{<kl>} - \Gamma_{kl}^k \sigma^{<il>} &= 0, \\
 \frac{\partial q^k}{\partial x^k} + \Gamma_{kl}^k q^l &= 0, \\
 \frac{2}{5} \left(g^{ik} \frac{\partial q^j}{\partial x^k} + g^{jk} \frac{\partial q^i}{\partial x^k} + g^{ik} \Gamma_{kl}^j q^l + g^{jk} \Gamma_{kl}^i q^l \right) &= \frac{1}{\tau} \sigma^{<ij>}, \\
 5p g^{ik} \frac{k_B}{m} \frac{\partial T}{\partial x^k} - 7\sigma^{<ik>} \frac{k_B}{m} \frac{\partial T}{\partial x^k} - 2 \frac{k_B}{m} T \left(\frac{\partial \sigma^{<ik>}}{\partial x^k} + \Gamma_{kl}^i \sigma^{<kl>} + \Gamma_{kl}^k \sigma^{<il>} \right) \\
 &= -\frac{2}{\tau} q^i.
 \end{aligned} \tag{4.4}$$

Here g_{ik} is the metric tensor, Γ_{jk}^i are the Christoffel symbols appropriate to the coordinates x^k .

For the planar case with rectangular Cartesian coordinates, g^{ik} is the Kronecker tensor and all Christoffel symbols vanish. In the cylindrical case with coordinates $(x^1, x^2, x^3) = (r, \vartheta, z)$ we have

$$g^{ik} = \begin{pmatrix} 1 & 0 \\ 0 & \frac{1}{r^2} \\ 0 & 0 & 1 \end{pmatrix} \text{ and } \Gamma_{22}^1 = -r, \quad \Gamma_{21}^2 = \Gamma_{12}^2 = \frac{1}{r}, \quad \Gamma_{kn}^m = 0 \text{ else.} \tag{4.5}$$

And in the spherical case with $(x^1, x^2, x^3) = (r, \vartheta, \varphi)$ we have

$$g^{ik} = \begin{pmatrix} 1 & 0 \\ \frac{1}{r^2} & \\ 0 & \frac{1}{r^2 \sin^2 \vartheta} \end{pmatrix} \text{ and } \Gamma_{31}^3 = \Gamma_{13}^3 = \Gamma_{21}^2 = \Gamma_{12}^2 = \frac{1}{r}, \Gamma_{22}^1 = -r, \\ \Gamma_{33}^1 = -r \sin^2 \vartheta, \Gamma_{32}^3 = \Gamma_{23}^3 = \text{ctg } \vartheta, \\ \Gamma_{33}^2 = -\sin \vartheta \cos \vartheta, \\ \Gamma_{kn}^m = 0 \quad \text{else.} \quad (4.6)$$

Note that, in all three cases, the coordinate lines are orthogonal so that the metric tensors are diagonal.

4.2.1.1 One Dimensional Solutions and Their Comparison with the Solutions Derived from the Navier-Stokes Fourier Theory

We investigate solutions, in which all fields depend on x^1 only and in which q^1 is the only non-vanishing component of the heat flux. In such a case, the Eq. (4.4) readily imply that all shear stresses vanish and that the deviatoric normal stresses are related to q^1 by

$$\sigma^{<11>} = -\frac{4}{5} \Gamma_{k1}^k \tau q^1, \sigma^{<22>} = \frac{4}{5} g^{22} \Gamma_{21}^2 \tau q^1, \sigma^{<33>} = \frac{4}{5} g^{33} \Gamma_{31}^3 \tau q^1. \quad (4.7)$$

We also obtain

$$\frac{dq^1}{dx^1} = -\Gamma_{k1}^k q^1. \quad (4.8)$$

We conclude from (4.4) that $p = \text{const.}$ holds and the 1-component provides a relation between the heat flux and the temperature gradient, viz.

$$q^1 = -\kappa \left(1 - \frac{7}{5} \frac{\sigma^{<11>}}{p} \right) \frac{dT}{dx^1}, \quad (4.9)$$

where κ is the heat conductivity related to the relaxation time τ by

$$\kappa = \frac{5}{2} \frac{k_B}{m} \tau p.$$

From (4.7), we conclude that, in spherical coordinates, the physical components of the shear stress are not zero. This result is particular to extended thermodynamics,

because with the Navier-Stokes constitutive equations we have $\sigma^{<ij>} = 0$ in any geometry. Thus we conclude, from (4.7), that in the planar case, where $\sigma^{<11>}$ vanishes, Fourier's law with a constant heat conductivity is recovered, because the heat flux is proportional to the gradient of the temperature. In the other cases, the cylindrical and the spherical ones, Fourier's law is not valid because of the second term on the right hand side of (4.7).

We now solve the system of equations and obtain the fields $\sigma^{<11>}$, q^1 , and T . The only geometric quantity left in that system is Γ_{k1}^k which reads

$$\Gamma_{k1}^k = \frac{j}{x^1} \quad \text{with } j = \begin{cases} 0 & \text{planar} \\ 1 & \text{for the cylindrical case.} \\ 2 & \text{spherical} \end{cases} \quad (4.10)$$

The general integral is easily obtained. In the planar case we have the simple solution

$$q^1 = c_1; \quad \sigma^{<11>} = 0, \quad T = c_2 - \frac{c_1}{\kappa} x^1 \quad (4.11)$$

with a linear temperature profile which is also predicted by the Fourier theory (c_1, c_2 are integration constants). For $j = 1, 2$ we have (we write now for evident reasons $r, q^r, \sigma^{<rr>}$ instead of $x^1, q^1, \sigma^{<11>}$)

$$q^r = \frac{c_1}{r^j} \quad \text{and} \quad \sigma^{<rr>} = -\frac{8j}{25} \frac{m}{k_B} \frac{\kappa}{p} \frac{c_1}{r^{j+1}},$$

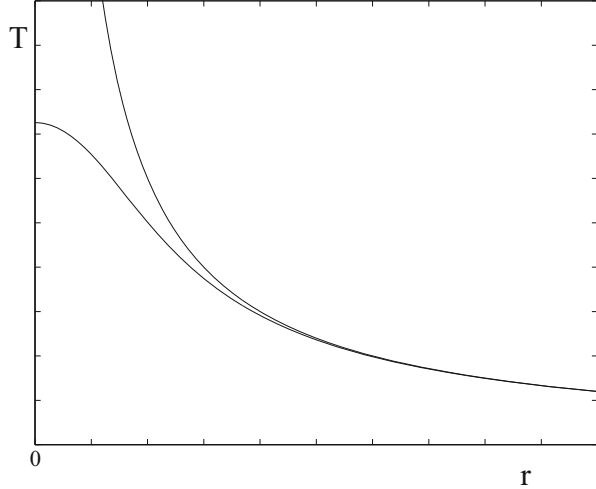
and (4.9) becomes

$$\frac{dT}{dr} = -\frac{c_1}{\kappa} \frac{r}{\frac{56}{125} j \frac{m}{k_B} \frac{\kappa}{p^2} c_1 + r^{j+1}}. \quad (4.12)$$

The first term in the denominator is absent in the Navier-Stokes Fourier theory, because $\sigma^{<rr>} = 0$ in that theory.

Thus we can see a first difference between ET and the Fourier theory: The derivative of the temperature tends to zero for $r \rightarrow 0$, while in the Fourier case it diverges. The general solution of (4.12) reads

Fig. 4.1 The behavior of the general integral of the temperature in the spherical symmetry. The divergent curve represents the solution of the Fourier theory while the bounded one represents the 13-moment solution



in the cylindrical case, i.e., for $j = 1$

$$T = c_2 - \frac{c_1}{2\kappa} \log(b + r^2),$$

in the spherical case, i.e., for $j = 2$

(4.13)

$$T = c_2 + \frac{c_1}{3 \cdot 2^{\frac{1}{3}} b^{\frac{1}{3}} \kappa} \left\{ \sqrt{3} \arctan \left(\frac{b^{\frac{1}{3}} - 2^{\frac{2}{3}} r}{\sqrt{3} b^{\frac{1}{3}}} \right) + \log \left(2 b^{\frac{1}{3}} + 2^{\frac{2}{3}} r \right) - \frac{1}{2} \log \left(2 b^{\frac{2}{3}} - 2^{\frac{2}{3}} b^{\frac{1}{3}} r + 2^{\frac{1}{3}} r^2 \right) \right\},$$

while according to the Fourier law we have

$$T = c_2 - \frac{c_1}{\kappa} \log r \quad \text{for } j = 1 \quad \text{and} \quad T = c_2 + \frac{c_1}{\kappa} \frac{1}{r} \quad \text{for } j = 2. \quad (4.14)$$

For abbreviation we have set $b = \frac{56}{125} \frac{m}{k_B} \frac{\kappa}{p^2} c_1$.

Figure 4.1 illustrates the difference between these solutions in the spherical case for c_1 arbitrarily assigned and c_2 such that the temperature vanishes for large values of r . We see that the temperature is finite in ET, while it diverges in the Fourier theory. We also observe that the solutions coincide when the gradient is small, while they differ significantly where the curves become steeper. As a matter of course, ET becomes relevant when gradients are large.

4.2.1.2 Solution of a Boundary Value Problem

In the planar case, the result from the Fourier theory is identical to the one from ET. Indeed, from (4.11)₃, we conclude that the temperature is linear in x^1 . More interesting are the radially symmetric cases, in particular, the cylindrically symmetric one.

We consider a gas between two co-axial cylinder or between two concentric spheres with inner radius r_i and outer radius r_e . We heat the gas at the inner radius with a prescribed heat flux q and the temperature at the outer radius is kept to a value T_e . Thus we solve the boundary value problem:

$$q^r(r_i) = q \quad \text{and} \quad T(r_e) = T_e. \tag{4.15}$$

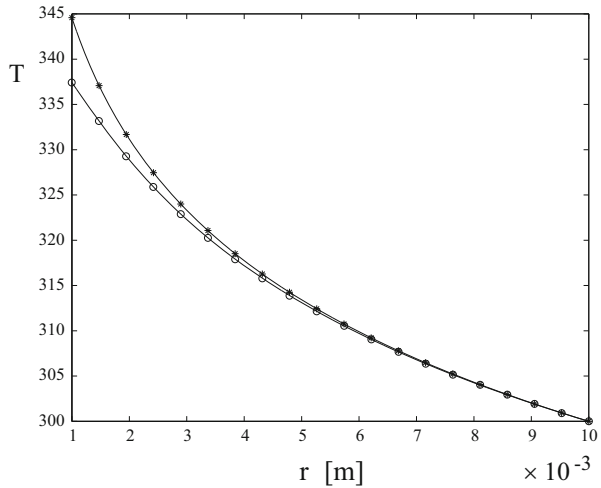
In the cylindrical case we obtain the solution:

$$q^r = \frac{qr_i}{r}, \quad \sigma^{rr} = \frac{8}{25} \frac{m}{k_B} \frac{\kappa}{p} \frac{qr_i}{r^2}, \quad T = T_e - \frac{qr_i}{2\kappa} \log \left(\frac{\frac{56}{125} \frac{m}{k_B} \frac{\kappa}{p^2} qr_i + r^2}{\frac{56}{125} \frac{m}{k_B} \frac{\kappa}{p^2} qr_i + r_e^2} \right). \tag{4.16}$$

Figure 4.2 shows this solution for T in the case of argon with the relative atomic mass $M = 40$ and for the data:

$$\begin{aligned} r_i &= 10^{-3} \text{ m}, \quad r_e = 10^{-2} \text{ m}, \quad p = 10^2 \frac{\text{N}}{\text{m}^2}, \\ \tau &= 10^{-5} \text{ s}, \quad q = 10^4 \frac{\text{W}}{\text{m}^2}, \quad T_e = 300 \text{ K}. \end{aligned} \tag{4.17}$$

Fig. 4.2 The behavior of the temperatures in the cylindrical case with the boundary data (4.17). Fourier theory (*stars*); 13-moment theory (*circles*)



The curve marked by circles in Fig. 4.2 represents the solution of ET and the one marked by stars is the solution of the Fourier theory. At the inner cylinder, the values of the two theories differ by 7.17 K.

In the spherical case we obtain with $b = \frac{56}{125} \frac{m}{k_B} \frac{\kappa}{p^2} q r_i^2$:

$$q^r = \frac{q r_i^2}{r^2}, \quad \sigma^{rr} = \frac{16}{25} \frac{m}{k_B} \frac{\kappa}{p} \frac{q r_i^2}{r^3},$$

$$T = T_e + \frac{c_1}{3 \cdot 2^{\frac{1}{3}} b^{\frac{1}{3}} \kappa} \left\{ \sqrt{3} \left[\arctan \left(\frac{b^{\frac{1}{3}} - 2^{\frac{2}{3}} r}{\sqrt{3} b^{\frac{1}{3}}} \right) - \arctan \left(\frac{b^{\frac{1}{3}} - 2^{\frac{2}{3}} r_e}{\sqrt{3} b^{\frac{1}{3}}} \right) \right] + \right. \quad (4.18)$$

$$\left. + \log \left(\frac{2 b^{\frac{1}{3}} + 2^{\frac{2}{3}} r}{2 b^{\frac{1}{3}} + 2^{\frac{2}{3}} r_e} \right) - \frac{1}{2} \log \left(\frac{2 b^{\frac{2}{3}} - 2^{\frac{2}{3}} b^{\frac{1}{3}} r + 2^{\frac{1}{3}} r^2}{2 b^{\frac{2}{3}} - 2^{\frac{2}{3}} b^{\frac{1}{3}} r_e + 2^{\frac{1}{3}} r_e^2} \right) \right\}.$$

Both solutions (4.16) and (4.18) hold in the interval $r_i \leq r \leq r_e$.

The case of co-axial cylinders should be easy to set up experimentally. Indeed, the inner cylinder could be realized by a wire and the heating may be effected by letting an electric current run through that wire. On the other hand the corresponding case of two concentric spheres may be quite difficult to realize experimentally.

4.2.2 *Difficulty in the ET Theory in a Bounded Domain When the Number of Fields is More Than 13*

In the above subsection, we have seen that the 13-moment ET theory predicts the new and interesting results that show an appreciable difference from the results predicted by the Navier-Stokes Fourier theory. We understand that, when there exists a steep gradient (and/or a rapid change), the ET theory is superior to the conventional classical TIP theory. Therefore it was natural that several authors tried to understand more deeply nonequilibrium phenomena in a bounded domain by using the ET theory with more than 13 moments. However, in such studies, the authors encountered a conceptually difficult problem. This is the problem of the boundary conditions.

All quantities in the 13-moment theory have concrete physical meanings and are observable. However, the quantities expressed by higher moments have not definite physical meanings and are, in general, impossible to be measured in experiments. Therefore we cannot pose the values of these quantities at the boundary of a domain, that is, we cannot pose the boundary conditions for the ET theory with more than 13 moments appropriately.

We may have a question: Is it really necessary to know all the boundary values? Indeed let us consider, for example, heat conduction in a gas filled in between two parallel plates. In this case, we need not know all boundary values except for, say, the temperatures at the two plates in order to study the phenomena experimentally. This

consideration seems to lead us to the following conjecture: if the temperature are fixed at the both sides, the other quantities adjust by themselves and have appropriate boundary values that are consistent with the experimental data. Such quantities are sometimes called uncontrollable quantities.

If this conjecture is true, we further want to know the mechanism of the self-adjustment. Several studies have been done. Struchtrup and Weiss [8] proposed the minimax principle for the entropy production, according to which the boundary values of the uncontrollable quantities are fixed. Barbera et al. also studied this problem [9]. They assume that the uncontrollable quantities fluctuate around the most probable values, and then they assume that the boundary values of the quantities are given by these most probable values.

Another strategy was proposed by Ruggeri and Lou [10]. Their approach is purely phenomenological. Let us consider the heat conduction problem again as an example with a mixture of gas. In order to obtain the temperature profile, they impose not only the boundary conditions but also some conditions inside a gas that should be given by experiments. The latter conditions are, for example, the temperatures at several points inside a gas. (See Sect. 16.6.2.)

Moreover, as pointed out by Brini and Ruggeri [11], there is another subtle problem. They proved that, if nonequilibrium variables have small values of the same order, then some derivative of these variables (critical derivatives) are not necessarily of the same order. As a consequence, the solutions violate the entropy principle and the system becomes to be inconsistent with the near-equilibrium approximation adopted.

Kinetic-theoretical study by using the concept of the accommodation factor may be helpful to solve this problem (see, for example, [12–16]). The accommodation factor is defined as the ratio between the effects of specular reflection and thermalized (diffuse) reflection of an incident molecule at the boundary wall. The introduction of this factor implies that the interaction between a gas and a boundary wall should be properly taken into consideration in order to fix the boundary conditions.

In conclusion, except for the 13-moment ET theory, the problem of the boundary conditions in ET in general still remains as a big issue to be solved even in the case of monatomic gases.

4.3 Molecular RET for Large Number of Moments

For rarefied gases, we have discovered that, in highly nonequilibrium phenomena such as sound waves with high frequencies, light scattering with large scattering angle, shock waves with large Mach number, predictions of the 13-moment theory are still not quite satisfactory when compared with experimental data although the 13-moment theory gives us better results compared with the Navier-Stokes Fourier theory. For such phenomena, we need a theory with more moments. In these cases, it is too difficult to proceed within a purely macroscopic theory like the 13-field RET

theory. Therefore let us recall that the fields F' s can be regarded as the moments of a distribution function f . In order to explain this approach by using the moments F' s, we first rewrite the hierarchy of balance laws in more compact notation:

$$\partial_t F_A + \partial_i F_{iA} = P_A, \quad (4.19)$$

with

$$F_A = \int_{R^3} m f c^A d\mathbf{c}, \quad F_{iA} = \int_{R^3} m f c_i c^A d\mathbf{c}, \quad (4.20)$$

$$P_A = \int_{R^3} Q c^A d\mathbf{c}, \quad (4.21)$$

where

$$c^A = \begin{cases} 1 & \text{for } A = 0, \\ c_{i_1} c_{i_2} \cdots c_{i_A} & \text{for } 1 \leq A \leq N, \end{cases}$$

and

$$F_A = \begin{cases} F & \text{for } A = 0, \\ F_{i_1 i_2 \cdots i_A} & \text{for } 1 \leq A \leq N, \end{cases} \quad F_{iA} = \begin{cases} F_i & \text{for } A = 0, \\ F_{i i_1 i_2 \cdots i_A} & \text{for } 1 \leq A \leq N. \end{cases} \quad (4.22)$$

The indices i and $i_1 \leq i_2 \leq \cdots \leq i_A$ are defined over $1, 2, 3$. In the followings, similar notations will be adopted.

Definition 4.1 A system of moments (4.19) truncated at the tensorial index N is called (N) -system. The (4.19) is called (N^-) -system if, for the last balance equation, we consider only the trace with respect to the two indexes, $F_{k_1 k_2 \cdots k_{N-2} l l}$, instead of the full N -order tensor $F_{k_1 k_2 \cdots k_{N-2} k_{N-1} k_N}$. If, instead of two indexes, we have the contraction with respect to two couples of two indexes, we add another minus: (N^{--}) .

According with this definition (that does not include all possible moment systems) the Euler fluid is a (2^-) -system and the Grad system is a (3^-) -system. Taking into account that all tensors are symmetric, the number n of moments, for an (N) -system, is given by

$$n_N = \frac{1}{6}(N+1)(N+2)(N+3), \quad (4.23)$$

and, for an (N^-) -system, is given by

$$n_{N^-} = \frac{1}{6}N(N^2 + 6N - 1). \quad (4.24)$$

4.3.1 Closure via the Entropy Principle

We require the compatibility of the truncated system (4.19) with the entropy law, i.e., all solutions of (4.19) must satisfy also the supplementary entropy balance law (1.22) where h^0, h^i and Σ are functionals of f [see (1.21)] through the moments (4.20) with $A = 0, \dots, N$. This is a strong restriction on the distribution function f , and now the problem to be solved is as follows: Determine the distribution function f_N under the condition that any classical solution of (4.19) with (4.20) and (4.21) is also the solution of (1.22).

For a generic entropy functional, which is valid not only for classical gases but also for degenerate gases such as Bose and Fermi gases, the following theorem was proved by Boillat and Ruggeri [17]:

Theorem 4.1 *Necessary and sufficient condition such that the truncated system of moments (4.19) satisfies an entropy principle (1.22) is that the truncated distribution function f_N depends on $(\mathbf{x}, t, \mathbf{c})$ only through a single variable:*

$$f_N \equiv f_N(\chi_N),$$

where

$$\chi_N = \sum_{A=0}^N u'_A(\mathbf{x}, t) c^A$$

is a polynomial in \mathbf{c} with the coefficients u'_A :

$$u'_A = \begin{cases} u' & \text{for } A = 0, \\ u'_{i_1 i_2 \dots i_A} & \text{for } 1 \leq A \leq N. \end{cases}$$

The entropy density, flux and production have the following expressions:

$$h^0 = m \int_{R^3} (\chi_N \Omega'(\chi_N) - \Omega(\chi_N)) d\mathbf{c}, \quad (4.25)$$

$$h^i = m \int_{R^3} c^i (\chi_N \Omega'(\chi_N) - \Omega(\chi_N)) d\mathbf{c}, \quad \Sigma = m \int_{R^3} Q \chi_N d\mathbf{c},$$

where the partition function $\Omega(\chi_N)$ satisfies the relation:

$$\Omega' = \frac{d\Omega}{d\chi_N} = f_N(\chi_N).$$

The system (4.19) becomes symmetric in the form (2.11) with the main field u'_A and potentials

$$h'^0 = m \int_{R^3} \Omega(\chi_N) d\mathbf{c}, \quad h'^i = m \int_{R^3} \Omega(\chi_N) c_i d\mathbf{c}, \quad (4.26)$$

provided $\Omega''(\chi_N) < 0$.

The proof can be made by the following general symmetrization Theorem 2.1. In fact (2.15) becomes in this case

$$F_A = \frac{\partial h'^0}{\partial u'_A}, \quad F_{iA} = \frac{\partial h'^i}{\partial u'_A},$$

then

$$dh'^0 = \sum_{A=0}^N F_A du'_A = m \int_{R^3} f \sum_{A=0}^N c_A du'_A d\mathbf{c} = m \int_{R^3} f d\chi_N d\mathbf{c} = d \int_{R^3} m\Omega(\chi_N) d\mathbf{c},$$

and (4.26)₁ hold. From (2.14) follows the (4.25). Analogous considerations are given for h'^i and h^i .

Then the original system of the moments becomes to be closed and to be symmetric hyperbolic in terms of the main-field components (2.11) (we omit now the summation on the repeated index B):

$$J_{AB} \partial_t u'_B + J_{iAB} \partial_i u'_B = P_A(u'_C), \quad A = 0, \dots, N \quad (4.27)$$

where

$$J_{AB}(u'_C) = \frac{\partial^2 h'^0}{\partial u'_A \partial u'_B} = \int_{R^3} m\Omega''(\chi_N) c^A c^B d\mathbf{c},$$

$$J_{iAB}(u'_C) = \frac{\partial^2 h'^i}{\partial u'_A \partial u'_B} = \int_{R^3} m\Omega''(\chi_N) c_i c^A c^B d\mathbf{c}.$$

Here and hereafter, the summation symbol with respect to A and/or B is omitted for simplicity. Indeed, the matrix J_{AB} is negative definite provided that $\Omega''(\chi_N) < 0$ holds, since

$$J_{AB} X_A X_B = \int_{R^3} m\Omega''(c^A X_A)^2 d\mathbf{c} < 0 \quad \forall X_A \neq 0.$$

If we require that h^0 is the usual entropy density for non-degenerate gases, viz.

$$h^0 = -k_B \int_{R^3} f_N \ln f_N d\mathbf{c},$$

we obtain from (4.25)

$$\left(\chi_N + \frac{k_B}{m} \ln \Omega' \right) \Omega' - \Omega = 0,$$

and by differentiation we obtain

$$f_N(\chi_N) = e^{-1-m\chi_N/k_B}. \quad (4.28)$$

In the present case we have

$$J_{AB}(u'_C) = -\frac{m^2}{k_B} \int_{R^3} f_N c_A c_B d\mathbf{c}, \quad J_{iAB}(u'_C) = -\frac{m^2}{k_B} \int_{R^3} f_N c_i c_A c_B d\mathbf{c}. \quad (4.29)$$

In an equilibrium state, (4.28) reduces to the well-known Maxwellian distribution function. We observe that f_N is not a solution of the Boltzmann equation. But we have the conjecture (open problem) that, for $N \rightarrow \infty$, f_N tends to a solution of the Boltzmann equation.

4.3.2 Closure via the Maximum Entropy Principle

Instead of the method of the entropy principle, there is an alternative in the ET theory of moments for the determination of the phase density f_N . This is the method of maximization of the entropy under some constraints.

We have discussed the MEP in Sect. 1.5.5. In this section, we summarize the results in the case of monatomic gases (see [17] for more details). Let us treat firstly a general case where the entropy h^0 is a generic functional of f :

$$h^0 = \int_{R^3} \psi(f) d\mathbf{c}. \quad (4.30)$$

We ask for the phase density f_N that provides the maximum of h^0 under the constraints of fixed values F_A for the moments:

$$F_A = \int_{R^3} m f c^A d\mathbf{c}.$$

With the Lagrange multipliers λ_A , we form the expression:

$$\mathcal{L} = \int_{R^3} \psi(f) d\mathbf{c} + \lambda_A \left(F_A - m \int c^A f d\mathbf{c} \right), \quad (4.31)$$

and obtain the relation:

$$\delta \mathcal{L} = \int_{R^3} \left(\frac{d\psi}{df} - m \lambda_A c^A \right) \delta f d\mathbf{c} = 0.$$

Thus we have

$$\frac{d\psi}{df} = m\lambda_A c^A$$

as a necessary condition for an extremum. Hence it follows that f is a function of

$$\chi = \lambda_A c^A,$$

and that $\psi(f)$ has the form:

$$\psi(f) = m \left(\chi f - \int f d\chi \right). \quad (4.32)$$

Insertion of (4.32) into (4.30) gives exactly the same result as that from the entropy principle (4.25). Thus we conclude that *the maximization of the entropy leads to the same result as that from the entropy principle in molecular RET of moments [17]*. In particular, the Lagrange multipliers λ_A are identical to the main field components u'_A .

4.4 Maximum Characteristic Velocity in the Classical Theory

Characteristic velocities λ , in the propagation direction with the unit vector $\mathbf{n} \equiv (n^i)$, of the symmetric hyperbolic system (4.27) with (4.28) are eigenvalues of

$$K^{AB} = J_{iAB} n^i - \lambda J_{AB} = -\frac{m^2}{k_B} \int_{R^3} f(\chi) (\mathbf{c} \cdot \mathbf{n} - \lambda) c^A c^B d\mathbf{c}. \quad (4.33)$$

In particular, the wave speeds for disturbances propagating in an equilibrium state are eigenvalues of

$$\int_{R^3} f_M(\mathbf{c} \cdot \mathbf{n} - \lambda) c^A c^B d\mathbf{c}, \quad (4.34)$$

where f_M is the Maxwellian distribution function. As the integrals in (4.34) are known, it is easy to evaluate the maximum eigenvalues for increasing N .

Numerical results were obtained by Weiss [18] who obtained increasing value of the maximum characteristic velocity for increasing number of moments n that depends on the truncation index N through (4.23). For instance, for $n = 20$, $\lambda_{\max} = 1.8c_0$ and for $n = 15.180$, $\lambda_{\max} = 9.36c_0$, where λ_{\max} is the maximum characteristic velocity in equilibrium in units of the sound wave velocity. Therefore an interesting problem is: what is the limit of λ_{\max} as $N \rightarrow \infty$?

4.4.1 Lower Bound Estimate and Characteristic Velocities for Large Number of Moments

In the previous examples, we have seen the validity of the subcharacteristic conditions. Now we are able to prove the behavior of λ_{\max} when $N \rightarrow \infty$. The $(k+1)(k+2)/2$ components of order k of the main field:

$$u'_{i_1 i_2 \dots i_k}, \quad i_1 \leq i_2 \leq \dots \leq i_k$$

can be mapped in the corresponding variables

$$u'_{pqr}, \quad p + q + r = k,$$

where p, q, r are, respectively, the number of indices over 1, 2, 3. With this notation

$$\chi = \sum_{p,q,r} u'_{pqr} c_1^p c_2^q c_3^r, \quad 0 \leq p + q + r \leq N.$$

Theorem 4.2 (Boillat and Ruggeri [17]) *For any N we have the lower bound condition:*

$$\frac{\lambda_{\max}}{c_0} \geq \sqrt{\frac{6}{5} \left(N - \frac{1}{2} \right)} \quad (4.35)$$

where c_0 is the sound velocity. Therefore, λ_{\max} becomes unbounded when $N \rightarrow \infty$.

Sketch of the Proof By the use of the variable u'_{pqr} , the components of the matrix (4.34) are given by

$$\int_{R^3} f_M(c_i n^i - \lambda) c_1^{p+s} c_2^{q+t} c_3^{r+u} d\mathbf{c}.$$

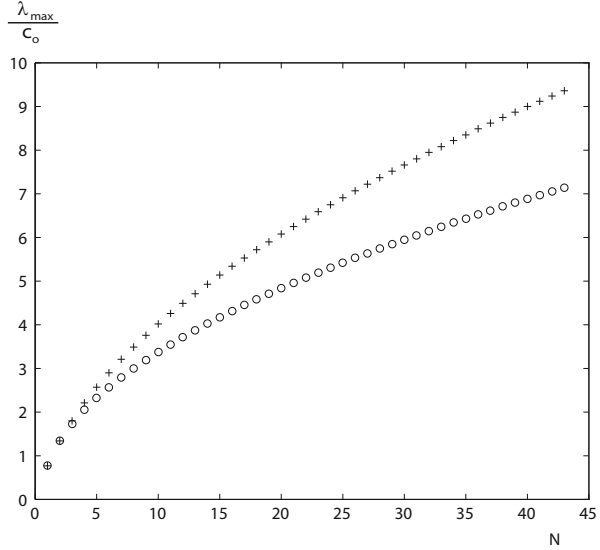
The matrix is negative semi-definite, if λ is the largest eigenvalue λ_{\max} . As the elements a_{ij} of a semi-definite matrix satisfy the inequalities:

$$a_{ii} a_{jj} \geq a_{ij}^2, \quad (4.36)$$

we have

$$\begin{aligned} & \int_{R^3} f_M(c_i n^i - \lambda_{\max}) c_1^{2p} c_2^{2q} c_3^{2r} d\mathbf{c} \int_{R^3} f_M(c_i n^i - \lambda_{\max}) c_1^{2s} c_2^{2t} c_3^{2u} d\mathbf{c} \\ & \geq \left(\int_{R^3} f_M(c_i n^i - \lambda_{\max}) c_1^{p+s} c_2^{q+t} c_3^{r+u} d\mathbf{c} \right)^2. \end{aligned} \quad (4.37)$$

Fig. 4.3 The behavior of the maximum characteristic velocity versus the truncation number N and the lower bound estimate (4.35)



In this case (4.37) reduces to

$$\begin{aligned} & \lambda_{\max}^2 \int_{R^3} f_M c_1^{2p} c_2^{2q} c_3^{2r} d\mathbf{c} \int_{R^3} f_M c_1^{2s} c_2^{2t} c_3^{2u} d\mathbf{c} \\ & \geq \left(\int_{R^3} f_M (c_1^i - \lambda_{\max}) c_1^{p+s} c_2^{q+t} c_3^{r+u} d\mathbf{c} \right)^2. \end{aligned} \tag{4.38}$$

With the choice $p = N, s = N - 1, q = r = t = u = 0, \mathbf{n} \equiv (1, 0, 0)$, this inequality becomes

$$\lambda_{\max}^2 \geq \frac{\int_{R^3} f_M c_1^{2N} d\mathbf{c}_1}{\int_{R^3} f_M c_1^{2(N-1)} d\mathbf{c}_1} = \frac{1}{b} \frac{\Gamma(N + 1/2)}{\Gamma(N - 1/2)} = \frac{6}{5} c_0^2 \left(N - \frac{1}{2} \right)$$

and the proof is completed. Therefore

$$\lim_{N \rightarrow \infty} \lambda_{\max} = \infty.$$

In Fig. 4.3, we compare the numerical values of λ_{\max}/c_0 given by Weiss [18] with our lower bound in the right-hand side of (4.35).

This is a surprising result because the first motivation of ET was to repair the paradox of infinite velocity of the Navier-Stokes Fourier classical approach. Therefore, for any finite N , we have symmetric hyperbolic systems with finite characteristic velocities. But when we take infinite moments we have a parabolic behavior.

Instead, in the relativistic context, it was proved that the limit of the maximum characteristic velocity for $N \rightarrow \infty$ is the light velocity [19–21] (see Sect. 4.7.1.1).

4.5 Convergence Problem and a Theory Near Equilibrium State

All results explained above are valid also for a case far from equilibrium provided that the integrals in (4.20) and (4.21) are convergent. The problem of the convergence of the moments is one of the main questions in a far-from-equilibrium case. In particular, as we will see, the index of truncation N must be even. This implies, in particular, that a theory with 13 moments is not allowed when far from equilibrium!

Moreover, if the conjecture that the distribution function f_N , when $N \rightarrow \infty$, tends to the distribution function f that satisfies the Boltzmann equation is true, we need another convergence requirement.

These problems were studied by Boillat and Ruggeri in [17]. As before, χ_N is expressed as

$$\chi_N = \sum_{p,q,r} u'_{pqr} c_1^p c_2^q c_3^r, \quad 0 \leq p + q + r \leq N. \tag{4.39}$$

Since

$$\left| \sum_{p,q,r} u'_{pqr} c_1^p c_2^q c_3^r \right| \leq a_N c^N$$

with

$$a_N = \max_{|\mathbf{t}|=1} v_N(\mathbf{t}), \quad v_N(\mathbf{t}) = \sum_{p,q,r} u'_{pqr} t_1^p t_2^q t_3^r,$$

when $p + q + r = N \rightarrow \infty$, the series is absolutely convergent for any c provided that

$$u'_{pqr} \rightarrow 0, \quad \frac{a_{N+1}}{a_N} \rightarrow 0.$$

Hence the components of the main field become smaller and smaller when N increases. This justifies the truncation of the system. On the other hand, when N is finite, the integrals of moments must also be convergent. When c is large, $\chi_N \simeq |c|^N v_N$. Therefore it is easy to see, by using the spherical coordinates, that the integrals of moments converge provided that $v_N(\mathbf{t}) < 0$ for any unit vector \mathbf{t} . But, as $v_N(-\mathbf{t}) = (-1)^N v_N(\mathbf{t})$, we can conclude that N must be even and $\max_{|\mathbf{t}|=1} v_N(\mathbf{t}) < 0$.

Now, the distribution function (4.28) obtained as the solution of the variational problem is expanded in the neighborhood of a local equilibrium state:

$$f_N \approx f_M \left(1 - \frac{m}{k_B} \tilde{u}'_A c_A \right), \quad \tilde{u}'_A = u'_A - u_A^E, \quad (4.40)$$

where u_A^E are the main field components evaluated in the local equilibrium state and f_M is the Maxwellian equilibrium distribution function. Taking into account the fact that all the equilibrium components of the main field vanish except those corresponding to the first five moments [see (2.29)] and plugging (4.40) into (4.20)₁, we obtain a linear algebraic system that permits to evaluate the main field \tilde{u}'_A in terms of the densities F_A :

$$J_{AB}^{\mathcal{M}} \tilde{u}'_B = F_A - F_A^E,$$

where F_A^E denotes the moments F_A evaluated in the equilibrium state and

$$J_{AB}^{\mathcal{M}} = -\frac{m^2}{k_B} \int_{R^3} f_M c_A c_B d\mathbf{c}. \quad (4.41)$$

And, by inserting \tilde{u}'_A just obtained above into (4.20)₂ and (4.21), the explicit dependence of the truncated fluxes and source terms on the densities is obtained. Finally, the truncated (N)-system becomes a closed system for the densities F_A .

The generalization of this procedure to higher order expansions of the distribution function has been given in [11] and as we will see in Chap. 12 there exists an interesting model in which we can close the system also far from equilibrium. This is the case of the 6-moment theory of polyatomic gases [22].

4.6 Comparison with Experimental Data: Sound Waves and Light Scattering

The ET theory is successful when the results are compared with experimental data, in particular, the results of sound waves with high frequencies and light scattering. In Fig. 4.4, taken from the book [4], we can see that the so-called dynamic factor $S(x, y)$ obtained by the ET theory fits very well the experimental data on light scattering (represented in the figure by dots) when N is sufficiently large.

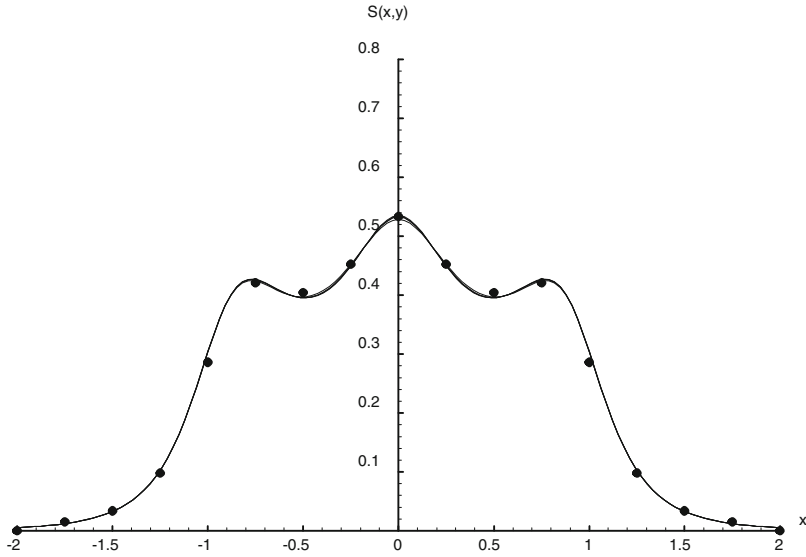


Fig. 4.4 Dynamical factor: the perfect agreement between the ET theory and the experimental data [4]

4.7 Relativistic Theory and the Limit of Maximum Characteristic Velocity

In the relativistic kinetic theory of rarefied gases, the phase density $f(x^\alpha, p^\alpha)$ ($\alpha = 0, 1, 2, 3$) satisfies the Boltzmann-Chernikov-Lichnerowicz-Marrot equation:

$$p^\alpha \partial_\alpha f = Q, \tag{4.42}$$

where x^α and p^α are the space-time coordinates and the four-momentum of an atom, respectively. We have $p_\alpha p^\alpha = (p^0)^2 - \mathbf{p}^2 = m^2 c^2$, $\mathbf{p}^2 = (p^1)^2 + (p^2)^2 + (p^3)^2$, where m is the atomic rest mass and c the speed of light. The right-hand side of (4.42) is due to collision between the atoms. Upon multiplication by p^A ($A = 0, 1, 2, \dots$)

and integration, (4.42) provides an infinite system of balance equations:

$$\left\{ \begin{array}{l} \partial_\alpha F^\alpha = 0, \\ \partial_\alpha F^{\alpha\alpha_1} = 0, \\ \partial_\alpha F^{\alpha\alpha_1\alpha_2} = P^{\alpha_1\alpha_2}, \\ \partial_\alpha F^{\alpha\alpha_1\alpha_2\alpha_3} = P^{\alpha_1\alpha_2\alpha_3}, \\ \vdots \\ \partial_\alpha F^{\alpha\alpha_1\dots\alpha_n} = P^{\alpha_1\alpha_2\dots\alpha_n}, \\ \vdots \end{array} \right. \quad (4.43)$$

or briefly:

$$\partial_\alpha F^{\alpha A} = P_A, \quad A = 0, 1, 2, \dots \quad (4.44)$$

for the moments $F^{\alpha A}$ and productions P_A given by

$$F^{\alpha A}(x^\beta) = \int p^\alpha p^A f d\mathbf{p}, \quad (4.45)$$

$$P_A(x^\beta) = \int Q p^A f d\mathbf{p}, \quad (4.46)$$

where A is a multindex:

$$p^A = \begin{cases} 1 & \text{for } A = 0 \\ p^{\alpha_1} p^{\alpha_2} \dots p^{\alpha_A} & \text{for } A \geq 1 \end{cases} \quad (4.47)$$

$$F^{\alpha A} = \begin{cases} F^\alpha & \text{for } A = 0 \\ F^{\alpha\alpha_1\dots\alpha_A} & \text{for } A \geq 1 \end{cases} \quad (4.48)$$

$$P_A = \begin{cases} 0 & \text{for } A = 0 \\ P^{\alpha_1\dots\alpha_A} & \text{for } A \geq 1 \end{cases} \quad (4.49)$$

and $0 \leq \alpha_1 \leq \alpha_2 \leq \dots \leq \alpha_A \leq 3$. We recall that the first five equations of (4.44) are the conservation laws of mass, momentum and energy, according to which the first five productions vanish: $P_A = 0$ for $A = 0, 1$. The volume element of the momentum space is given by $d\mathbf{p} = \sqrt{-g} dp^1 dp^2 dp^3 / p^0$ and the integrals, which are supposed to be convergent, are taken over the whole \mathbf{p} -space.

We introduce the quantity:

$$h^\alpha = -k_B \int p^\alpha \{ (s^2 - 1 + \ln f) f + s(1 - sf) \ln(1 - sf) \} d\mathbf{p} \quad (4.50)$$

where $s = 0, -1, 1$ correspond, respectively, to the non-degenerate gas, the Fermi gas and the Bose gas. It is well known that we obtain, from (4.42), the supplementary inequality:

$$\partial_\alpha h^\alpha = \Sigma \geq 0. \quad (4.51)$$

This expression suggests the balance of entropy when we identify h^α and Σ with the four-entropy vector and the entropy production, respectively. Then (4.51) expresses the famous H-theorem in the relativistic framework.

4.7.1 Finite System of Moment Equations and Its Closure

We now consider a finite system of moment equations with the tensorial index $A = 0, \dots, N$. In this case, as in the classical case, we can accomplish the closure of the system by using the entropy principle or the variational method of the maximum entropy principle (Boillat and Ruggeri [19, 20]). We obtain

$$f_N = \frac{1}{e^{-\chi/k_B} + s}, \quad (4.52)$$

where

$$\chi = u'_A p^A. \quad (4.53)$$

The system is closed in terms of the main field components u'_A :

$$H^{\alpha AB}(u'_C) \partial_\alpha u'_B = P_A(u'_C), \quad A = 0, 1 \dots N \quad (4.54)$$

with the symmetric matrices

$$H^{\alpha AB} = \int \frac{\exp(-\chi/k_B)}{k_B (1 + s \exp(-\chi/k_B))^2} p^\alpha p^A p^B d\mathbf{p}. \quad (4.55)$$

$H^{\alpha AB} \zeta_\alpha$ is negative definite for any timelike vector ($\zeta_\alpha \zeta^\alpha > 0$). This implies that the system (4.54) is a symmetric hyperbolic system (in the sense of Friedrichs) and is local in time. Its Cauchy problem is well-posed.

4.7.1.1 Propagation in an Equilibrium State and the Maximum Characteristics Velocity

The wave surface $\phi(x^\alpha) = 0$ is a solution of the characteristic equation:

$$\det(H^{\alpha AB} \partial_\alpha \phi) = 0.$$

As a consequence, the four gradient $\partial_\alpha \phi$ cannot be timelike and therefore the velocities of waves cannot exceed the velocity of light, i.e., $\lambda \max \leq c$. When the number of equations increases, as was already shown, the maximum wave velocity cannot decrease. Now a question is: Does this velocity tend to c when N tends to infinity?

A thermodynamic equilibrium state is defined as the state for which the productions g^A vanish and the entropy production Σ reaches its minimum value, i.e., zero. According with the general result, all the main-field variables except for the first five variables are zero:

$$u' = -\frac{g}{T}, \quad u'_\alpha = \frac{u_\alpha}{T}, \quad (4.56)$$

where g , T and u_α are, respectively, the chemical potential, the absolute temperature, and the four-velocity. Therefore, for any truncation index N , the χ given by (4.53) reduces to $\chi/k_B = (-g + u_\alpha p^\alpha)/(k_B T)$ in an equilibrium state. And, in a case at rest where $u^i = 0$, $u^0 = c$, $p^0 = \sqrt{m^2 c^2 + \mathbf{p}^2}$ we have

$$\frac{\chi}{k_B} = -a + \gamma \sqrt{1 + \frac{\mathbf{p}^2}{m^2 c^2}},$$

where $a = g/k_B T$, $\gamma = mc^2/k_B T$. In this case, the distribution function reduces to the well-known Jüttner equilibrium distribution. We recall that for a Fermi gas a can assume all real values while for a Bose gas $a + \gamma > 0$.

The wave velocity λ in the direction of the normal \mathbf{n} to the wave front is an eigenvalue of

$$\det(H^{iAB} n_i - \lambda H^{0AB}) = 0. \quad (4.57)$$

The matrix in (4.57) is negative semidefinite for the maximum eigenvalue, that is, if we take $\mathbf{n} \equiv (1, 0, 0)$, the components of the matrix:

$$H^{iAB} - \lambda_{\max} H^{0AB} = \int \frac{df}{dx} p^A p^B (p^1 - \lambda p^0) d\mathbf{p}$$

satisfy the inequalities in the form $a_{ii} a_{jj} - a_{ij}^2 \geq 0$ [see (4.36)]. Therefore, choosing $p^A = (p^1)^n$, $p^B = (p^1)^{n-1}$, we have

$$\frac{\lambda_{\max}^2}{c^2} \int \frac{df}{d\chi} (p^1)^{2n} d^3 p \int \frac{df}{d\chi} (p^1)^{2(n-1)} d^3 p \geq \left(\int \frac{df}{d\chi} (p^1)^{2n} \frac{d^3 p}{p^0} \right)^2, \quad (4.58)$$

since the integrals of odd functions vanish.

By introducing the spherical coordinates, the above inequality, after some straightforward calculations, yields

$$\frac{\lambda_{\max}^2}{c^2} \geq \frac{2n-1}{2n+1} \frac{J_{n+1}^2}{I_n I_{n+1}}, \quad (4.59)$$

where

$$I_n = \int_0^\infty \phi(r)r^{2n} dr, \quad J_n = \int_0^\infty \frac{\phi(r)r^{2n}}{\sqrt{1+r^2}} dr,$$

$$\phi(r) = \frac{e^{\psi(r)}}{(1 + se^{\psi(r)})^2},$$

$$\psi(r) = \frac{\chi e}{k_B} = -a - \gamma \sqrt{1+r^2}, \quad s = 0, \pm 1.$$

Therefore we conclude that: *For any type of gas including the degenerate gases of fermions and bosons, the largest wave velocity has the lower and upper bounds.*

In the case of a non-degenerate gas, the previous integrals can be written in terms of the Bessel function of second kind and read

$$\frac{\lambda_{\max}^2}{c^2} \geq \frac{(2N-1) K_{N+1}(\gamma)}{\gamma K_{N+2}(\gamma)}, \quad (4.60)$$

where $\gamma = mc^2/(k_B T)$. Using the recurrence relation for Bessel functions $K_{N+2} - K_N = 2(N+1)K_{N+1}/\gamma$, we obtain that, for $N \rightarrow \infty$, the limit value of λ_{\max} in (4.59) is the light velocity c , since it has already been proved that it cannot be larger than c . Thus, *when the number of moments tends to infinity, the maximum velocity in equilibrium tends to the light velocity.*

This result can be proved also for degenerate gases because our proof is completely independent of the interaction term Q of (4.42).

In the *ultrarelativistic case* corresponding to small γ , taking the properties of the Bessel functions into account when $\gamma \rightarrow 0$, we obtain the simple inequality:

$$\frac{\lambda_{\max}^2}{c^2} \geq \frac{(2N-1)}{2(N+1)}.$$

4.7.2 The Macroscopic Relativistic 14-Field Theory

The most interesting case is the relativistic 14-moment ET theory developed by Liu et al. [23]. The system in this case coincides with the system obtained by kinetic considerations by C. Marle [24], which are similar to the ones of Grad:

$$\begin{cases} \partial_\alpha F^\alpha = 0, \\ \partial_\alpha F^{\alpha\beta} = 0, \\ \partial_\alpha F^{\alpha\beta\gamma} = P^{\beta\gamma}. \end{cases} \quad (4.61)$$

The field variables in this case are the number of particle vector F^α and the full energy-momentum tensor $F^{\alpha\beta} = T^{\alpha\beta}$, while $F^{\alpha\beta\gamma}$ and $Pi^{\beta\gamma}$ are constitutive functions of the field variables. By using the familiar variables (n particle number, e the energy density, $t^{<\alpha\beta>}$ the deviatoric viscous stress tensor, Π the dynamic pressure and q^α the heat flux four-vector), the following expressions are obtained [23]:

$$\begin{aligned} F^\alpha &= nm u^\alpha, \\ F^{\alpha\beta} &= t^{<\alpha\beta>} + (p + \Pi) h^{\alpha\beta} + \frac{1}{c^2} (u^\alpha q^\beta + u^\beta q^\alpha) + \frac{e}{c^2} u^\alpha u^\beta, \\ F^{\alpha\beta\gamma} &= (C_1 + C_2 \Pi) u^\alpha u^\beta u^\gamma + \\ &\frac{c^2}{6} (nm - C_1 + C_2 \Pi) (g^{\alpha\beta} u^\gamma + g^{\beta\gamma} u^\alpha + g^{\alpha\gamma} u^\beta) + \\ &C_3 (g^{\alpha\beta} q^\gamma + g^{\beta\gamma} q^\alpha + g^{\alpha\gamma} q^\beta) + C_4 (t^{<\alpha\beta>} u^\gamma + t^{<\beta\gamma>} u^\alpha + t^{<\alpha\gamma>} u^\beta). \end{aligned}$$

The main field becomes

$$\begin{aligned} u' &= -\frac{g}{T} - \tau_0 \Pi, \\ u'_\alpha &= \frac{u_\alpha}{T} - \tau_1 \Pi u_\alpha - \tau_2 q_\alpha, \\ u'_{\alpha\beta} &= -\tau_3 t_{<\alpha\beta>} - \tau_4 \Pi h_{\alpha\beta} - \frac{1}{c^2} \tau_5 (u_\alpha q_\beta + u_\beta q_\alpha) - \frac{3}{c^2} \tau_6 \Pi u_\alpha u_\beta, \end{aligned}$$

where $h^{\alpha\beta}$ is the projector and we omit the long expressions of the coefficients that appear in the previous equations.

If we put

$$u'_{\alpha\beta} = 0 \tag{4.62}$$

then we have:

$$t_{<\alpha\beta>} = 0, \quad q_\alpha = 0, \quad \Pi = 0, \tag{4.63}$$

and we obtain the equilibrium principal subsystem, i.e., the Euler relativistic fluid system:

$$\begin{cases} \partial_\alpha F^\alpha = 0, \\ \partial_\alpha F^{\alpha\beta} = 0 \end{cases} \tag{4.64}$$

with

$$F^\alpha = nm u^\alpha, \quad F^{\alpha\beta} = p h^{\alpha\beta} + \frac{e}{c^2} u^\alpha u^\beta. \tag{4.65}$$

4.7.2.1 Remark on the Einstein Equation

From the viewpoint of ET, we can see the Einstein equation in a different way. In fact, in the classical approach, the number of balance laws is usually five. Only one component (for example, the internal energy) in the energy-momentum tensor is considered as a field variable, and the remaining ones are prescribed by the constitutive equations. While, in ET, it is assumed that all the components of the energy-momentum tensor are field variables. Therefore, in ET, the Einstein equation:

$$R_{\mu\nu} - \frac{1}{2}g_{\mu\nu}R = -\frac{8\pi G}{c^4}T_{\mu\nu}$$

becomes a *universal* equation, independent of the constitution of the material [25].

For more details concerning RET of monatomic gases, interested readers can consult the book [4] and the survey papers [26, 27].

Finally we want to recall that many applications of ET not only to rarefied gases but also to other similar fields such as fluid-dynamic models in semiconductor physics (see for example [28–30]) have been made.

References

1. I.-S. Liu, I. Müller, Extended thermodynamics of classical and degenerate ideal gases. *Arch. Ration. Mech. Anal.* **83**, 285 (1983)
2. H. Grad, On the kinetic theory of rarefied gases. *Commun. Pure Appl. Math.* **2**(4), 331 (1949)
3. W. Dreyer, Maximization of the entropy in non-equilibrium. *J. Phys. A: Math. Gen.* **20**, 6505 (1987)
4. I. Müller, T. Ruggeri, *Rational Extended Thermodynamics*, 2nd edn. (Springer, New York, 1998)
5. T. Ruggeri, The entropy principle: from continuum mechanics to hyperbolic systems of balance laws. *Bollettino dell'Unione Matematica Italiana* (**8**)**8-B**, 1 (2005)
6. G. Boillat, T. Ruggeri, Hyperbolic principal subsystems: entropy convexity and subcharacteristic conditions. *Arch. Ration. Mech. Anal.* **137**, 305 (1997)
7. I. Müller, T. Ruggeri, Stationary heat conduction in radially, symmetric situations – an application of extended thermodynamics. *J. Non-Newtonian Fluid Mech.* **119**, 139 (2004)
8. H. Struchtrup, W. Weiss, Maximum of the local entropy production becomes minimal in stationary processes. *Phys. Rev. Lett.* **80**, 5048 (1998)
9. E. Barbera, I. Müller, D. Reitebuch, N. Zhao, Determination of boundary conditions in extended thermodynamics via fluctuation theory. *Continuum Mech. Thermodyn.* **16**, 411 (2004)
10. T. Ruggeri, J. Lou, Heat conduction in multi-temperature mixtures of fluids: the role of the average temperature. *Phys. Lett. A* **373**, 3052 (2009)
11. F. Brini, T. Ruggeri, Entropy principle for the moment systems of degree α associated to the Boltzmann equation. Critical derivatives and non controllable boundary data. *Continuum Mech. Thermodyn.* **14**, 165 (2002)
12. H. Struchtrup, Heat transfer in the transition regime: solution of boundary value problems for Grad's moment equations via kinetic schemes. *Phys. Rev. E* **65**, 041204 (2002)

13. H. Struchtrup, W. Weiss, Temperature jump and velocity slip in the moment method. *Continuum Mech. Thermodyn.* **12**, 1 (2000)
14. H. Struchtrup, *Macroscopic Transport Equations for Rarefied Gas Flow: Approximation Methods in Kinetic Theory* (Springer, Berlin/Heidelberg, 2005)
15. N. Zhao, M. Sugiyama, Analysis of heat conduction in a rarefied gas at rest with a temperature jump at the boundary by consistent-order extended thermodynamics. *Continuum Mech. Thermodyn.* **18**, 367 (2007)
16. S. Taniguchi, A. Iwasaki, M. Sugiyama, Relationship between Maxwell boundary condition and two kinds of stochastic thermal wall. *J. Phys. Soc. Jpn.* **77**, 124004 (2008)
17. G. Boillat, T. Ruggeri, Moment equations in the kinetic theory of gases and wave velocities. *Continuum Mech. Thermodyn.* **9**, 205 (1997)
18. W. Weiss, Zur Hierarchie der Erweiterten Thermodynamik. Dissertation, TU Berlin, 1990
19. G. Boillat, T. Ruggeri, Maximum wave velocity in the moments system of a relativistic gas. *Continuum Mech. Thermodyn.* **11**, 107 (1999)
20. G. Boillat, T. Ruggeri, Relativistic gas: moment equations and maximum wave velocity. *J. Math. Phys.* **40**, 6399 (1999)
21. F. Brini, T. Ruggeri, Maximum velocity for wave propagation in a relativistic rarefied gas. *Continuum Mech. Thermodyn.* **11**, 331 (1999)
22. T. Ruggeri, Non-linear maximum entropy principle for a polyatomic gas subject to the dynamic pressure. *Bull. Inst. Math. Acad. Sin. Special Issue in honor of Tai-Ping Liu 70 birthday.* **11** (2016)
23. I.-S. Liu, I. Müller, T. Ruggeri, Relativistic thermodynamics of gases. *Ann. Phys.* **169**, 191 (1986)
24. C. Marle, Sur l'établissement des équations de l'hydrodynamique des fluides relativistes dissipatifs I et II. *Ann. Inst. Henri Poincaré A* **10**, 67 (1969); *A* **10**, 127 (1969)
25. T. Ruggeri, *Relativistic Extended Thermodynamics: General Assumptions and Mathematical Procedure Corso CIME Noto (Giugno 1987)*, ed. by A. Anile, Y. Choquet-Bruhat. *Lecture Notes in Mathematics*, vol. 1385 (Springer, Berlin, 1989), pp. 269–277
26. I. Müller, Extended thermodynamics: a theory of symmetric hyperbolic field equations. *Entropy* **10**, 477 (2008)
27. T. Ruggeri, The entropy principle from continuum mechanics to hyperbolic systems of balance laws: the modern theory of extended thermodynamics. *Entropy* **10**, 319 (2008)
28. A.M. Anile, S. Pennisi, Thermodynamic derivation of the hydrodynamical model for charge transport in semiconductors. *Phys. Rev. B* **46**, 13186 (1992)
29. A.M. Anile, V. Romano, Non parabolic band transport in semiconductors: closure of the moment equations. *Continuum Mech. Thermodyn.* **11**, 307 (1999)
30. M. Trovato, L. Reggiani, Maximum entropy principle and hydrodynamic models in statistical mechanics. *Riv. Nuovo Cimento Soc. Ital. Fis.* **35**, 99 (2012)